

An integrative approach for modeling and simulation of Heterocyst pattern formation in Cyanobacteria strands

Alejandro Torres-Sánchez^{1,2}, Jesús Gómez-Gardeñes^{1,3}, Fernando Falo^{1,3,*}

1 Departamento de Física de la Materia Condensada, Universidad de Zaragoza, E-50009 Zaragoza, Spain.

2 Laboratori de Càlcul Numèric, Universitat de Politècnica de Catalunya, E-08034 Barcelona, Spain.

3 Instituto de Biocomputación y Física de Sistemas Complejos (BIFI), Universidad de Zaragoza, E-50018 Zaragoza, Spain.

* E-mail: fff@unizar.es

Abstract

A comprehensive approach to cellular differentiation in cyanobacteria is developed. To this aim, the process of heterocyst cell formation is studied under a systems biology point of view. By relying on statistical physics techniques, we translate the essential ingredients and mechanisms of the genetic circuit into a set of differential equations that describes the continuous time evolution of combined nitrogen, PatS, HetR and NtcA concentrations. The detailed analysis of these equations gives insight into the single cell dynamics. On the other hand, the inclusion of diffusion and noisy conditions allows simulating the formation of heterocysts patterns in cyanobacteria strains. The time evolution of relevant component concentrations are calculated allowing for a comparison with experiments. Finally, we discuss the validity and the possible improvements of the model.

Author Summary

Understanding the underlying mechanisms favoring the cooperative behavior exhibited by different cell types constitutes the first step to explain the emergence of specialized cells in the early life stages of multicellular systems. Multicellularity appeared on Earth some billion years ago, and cyanobacteria are one of the first organisms that developed this feature. In fact, being differentiation processes the cornerstone of multicellularity, cyanobacteria strands are paradigmatic examples of prokaryotic cellular differentiation and cooperative pattern formation. When a strand of cyanobacteria cells is deprived of combined nitrogen, some of the vegetative cells start differentiating into heterocysts, which are terminally differentiated nitrogen-fixing cells. However, not all vegetative cells differentiate as (*i*) heterocysts lose their photosynthetic capacity so they need vegetative cells around to be provided of a source of fixed carbon and (*ii*) cell division, i.e. reproduction, is only accomplished by vegetative cells. From such paradigmatic example it is clear that differentiation processes are the result of the interplay of complex regulatory networks acting inside the cell and external stimuli, from both the neighboring cells and the environment. Thus, in this article we present an integrative approach that combines the study of the internal regulatory processes, diffusion and noisy environments in order to capture the key mechanisms leading to the differentiation of vegetative cyanobacteria into heterocysts and the subsequent pattern formation.

Introduction

One of the most striking and complex problems tackled by biology is the formation of multicellular organisms. Multicellular organisms rely on cell differentiation, a mechanism by which cells become more specialized. More precisely, differentiation processes lead to precise alterations in gene expression that result in changes in cell morphology and function. These processes are highly dynamical, directed by complex regulatory networks involving cell-to-cell interactions, and often triggered by external stimuli. As a result of the differentiation, the organism separates functions in different cell types establishing a rich cooperative pattern that increases its complexity and adaptability. Due to the large number of scales involved, ranging from protein binding to diffusion of specific elements throughout the organism, a correct mathematical modeling of differentiation processes and biological pattern formation demands an integrated approach combining tools from statistical mechanics and the theory of dynamical systems (see for instance [1, 2]).

A landmark process of (prokaryotic) cellular differentiation and cooperative pattern formation is the heterocyst differentiation in cyanobacteria strands [3, 4]. Cyanobacteria are thought to be one of the first organisms in developing multicellularity some (2 – 3) billion years ago [5]. These bacteria perform oxygenic photosynthesis releasing oxygen to the environment. On the other hand, nitrogenase, the enzyme that performs nitrogen fixation, is deactivated by oxygen so that nitrogen fixation cannot occur in its presence [6]. Cyanobacteria solve the incompatibility of incorporating both oxygenic photosynthesis and nitrogen fixation by separating these processes (*i*) temporally, such as in the unicellular *Cyanothece sp.* strain ATCC 51142 that presents photosynthetic activity during the day and fixes nitrogen during the night [7], or (*ii*) spatially, by the generation of non-photosynthetic nitrogen-fixing cells.

When provided of combined nitrogen (such as nitrate, nitrite, ammonium or urea), most cyanobacteria (with *Anabaena* PCC strain 7120 the most representative example) form long filaments of photosynthetic vegetative cells. However, in the absence of combined nitrogen (cN), a part of the vegetative cells differentiate into heterocysts, which are terminally differentiated nitrogen-fixing cells. By differentiating, heterocysts lose their photosynthetic capacity, so they need for an external source of fixed carbon [8, 9]. To this aim, each forming heterocyst sends a signal, by means of the diffusion of some particular chemical along the chain, to its neighboring cells to avoid their differentiation. A cooperative pattern is thus established: heterocysts provide cN to the cellular chain while non-differentiated cells remain supplying fixed carbon to the system. As a result, heterocysts appear interspersed within around 10 vegetative cells, depending on the species, forming a semiregular pattern that remains approximately constant in the chain regardless cell division [4]. This pattern forms one of the simplest and most primitive examples of multicellular organism as a product of the interdependence between heterocysts and vegetative cells. Interestingly, an isolated cyanobacterium does not differentiate but it first divides so that one of the descendants differentiates. This is necessary since (*i*) a sole heterocyst would lack of a source of fixed carbon and (*ii*) it would not reproduce since it is a terminally differentiated cell [10].

Some quantitative modeling has been done to explain the dynamical and equilibrium properties of heterocyst pattern formation. In references [11, 12] Rutenberg and coworkers analyzed a model to explain heterocyst patterns by means of the study of combined nitrogen diffusion along a cyanobacterial strain. On the other hand, Gerdtzen *et al.* [13] modeled cyanobacterial filaments based on a time-discrete dynamical system exhibiting the main interactions between the most important proteins that take part in heterocyst formation.

In this work, we develop a simple mathematical model, by integrating the recent experimental results on the gene regulatory network of cyanobacteria into the theoretical machinery of system biology. To this aim, we take into account the fundamental genetic paths that underlie the differentiation of heterocysts considering the interactions that come into play in this process. Furthermore, our model connects the diffusion of combined nitrogen with the dynamical properties of the underlying genetic circuit of each cyanobacterium, linking pattern formation and maintenance. Our model shows that noise enables the

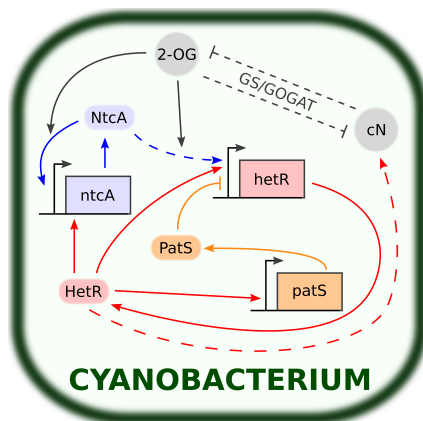


Figure 1. Main components and interactions involved in the reaction to nitrogen deprivation in cyanobacteria. Rectangular boxes represent genes (*ntcA*, *hetR* and *patS*) while rounded boxes and circles represent transcription factors (NtcA, HetR and PatS) and smaller molecules (2-OG and cN) respectively. Normal-tipped and flat-tipped arrows stand for up-regulating and down-regulating processes respectively. Dashed lines stand for indirect or imperfectly understood interactions. The accumulation of 2-OG enhances the DNA-binding activity of NtcA, which in turn up-regulates the transcription of *ntcA* and *hetR*. HetR activates *ntcA* and *hetR* (composing the central NtcA-HetR autoregulatory loop), the inhibitor *patS* and other genes that lead to nitrogen fixation and the morphological changes involved in heterocyst differentiation. 2-OG and cN levels are linked through the GS/GOGAT cycle (see Fig. 2).

development of the characteristic heterocysts patterns for a wide range of model parameters, revealing, in a quantitative way, that cyanobacteria strains may have evolved towards an efficient response mechanism to the noisy conditions that characterize the natural environment.

The work is structured as follows. First we present the main actors of the basic regulatory network and the different dynamical interactions that take place during the differentiation process. Then we develop a mathematical model for the unicellular reaction to nitrogen deprivation. Although a unicellular model does not suffice to understand heterocyst formation, we analyze the main features that arise from the dynamical behavior of the system to gain insight about cell dynamics under different external conditions. Finally, we round off the paper by introducing the spatial model consisting of a filament of cyanobacteria, each one characterized by the dynamical circuit developed previously, that interact by means of protein diffusion.

Results

Description of the main Genes and their basic Genetic Circuit

Heterocyst development begins with sensing combined-nitrogen (cN) limitation and ends with nitrogen fixation in mature heterocysts. This process is usually completed after a time of about 20 hours at 30°C [9]. In Fig. 1 we show a basic scheme of the genetic circuit including the most relevant elements and their respective interactions. Here we explain the main features of this genetic circuit.

The process is initiated with the accumulation of the enzyme 2-oxoglutarate (2-OG) as a consequence of nitrogen deprivation [9, 14]. 2-OG interacts with ammonium through the GS/GOGAT cycle [15–17] (see Fig. 2). Under cN starvation, the GS/GOGAT cycle breaks down, leading to the afore-mentioned

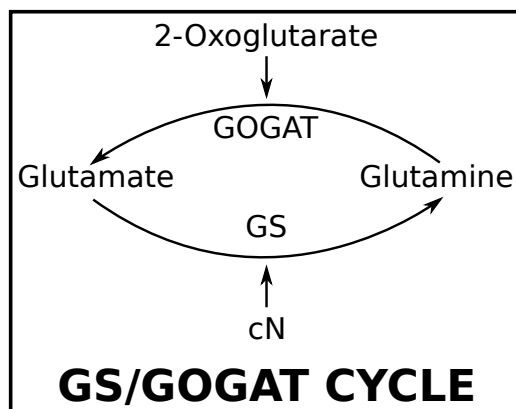


Figure 2. 2-OG and cN indirectly interact through the GS/GOGAT cycle. Glutamine is transformed into glutamate by means of 2-OG through the 2-OG amidotransferase (GOGAT) while cN converts glutamate into glutamine through the glutamine synthetase (GS). The importance of the cycle in heterocyst differentiation is twofold. From one side, it constitutes the early one-cell sensor to nitrogen starvation: the absence of cN breaks the cycle down and 2-OG starts to accumulate, whose action leads to the cascade of processes that provoke the differentiation (see Fig. 1). On the other hand, later during the differentiation, it process the cN created by the heterocysts decreasing the levels of 2-OG. The latter is crucial for the formation of the heterocyst pattern (see Fig. 3).

accumulation of 2-OG inside the cell [9]. In its turn, 2-OG stimulates the DNA-binding activity of NtcA, an important transcription factor for heterocyst development [16,18,19]. Furthermore, the transcription of the genes targeted by NtcA does not start in the absence of 2-OG [20,21]. NtcA presents an auto-regulatory activity [20,22,23] and indirectly activates the key gene that controls cell differentiation and pattern formation: *hetR* [24–26]. For its binding activity NtcA needs for homodimerization [27,28]. Therefore, the accumulation of 2-OG is the factor that triggers differentiation. In agreement with this idea, artificial increased levels of 2-OG result in heterocyst development even in the presence of ammonium [14,16,29].

As already mentioned, the next step of the genetic circuit is the activation of *hetR*. Importantly, null mutants of *hetR* do not produce heterocysts whereas an overexpression of *hetR* leads to an increased heterocyst frequency [25,30,31]. The transcription of *hetR* is induced by NtcA through the action of an intermediate, *nrrA* [26]. The DNA-binding activity of HetR requires its homodimerization [32,33]. Multiple transcription factors related to heterocyst formation are up-regulated by HetR, including *hetR* itself [33], *ntcA* [34] and *patS* [33].

The up-regulatory loop composed of NtcA and HetR is central for heterocyst differentiation [34–37]. However, the action of NtcA and HetR alone cannot account for pattern formation. Another transcription factor, PatS, inhibits the DNA-binding activity of HetR [8,33,38,39]. This inhibitory behavior is essential for the communication with adjacent cells and thus for achieving the observed patterns of vegetative cells and heterocysts in cyanobacteria strains (see Fig. 3). Furthermore, *patS* is strongly expressed in differentiating cells and mature heterocysts due to its upregulation by HetR [8]. A strain without *patS* develops multiple contiguous heterocysts (about a 30% of all cells as compared to the usual 10% in the wild-type strain). On the other hand, an overexpression of *patS* suppresses heterocyst differentiation [9]. In fact, the addition to the growth medium of a synthetic peptide composed of the last five residues (RGSGR) of PatS (PatS5) inhibits heterocyst development, suggesting that PatS5 may be a diffusive mature form of PatS that stops the differentiation of the rest of vegetative cells of the strain [38].

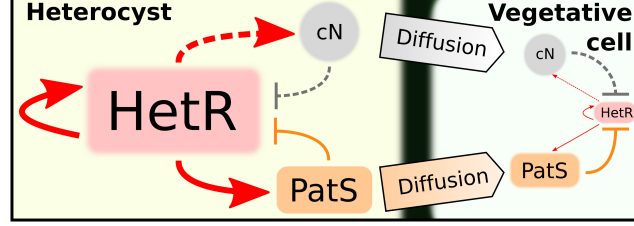


Figure 3. Schematic representation of the diffusion processes that sustain the heterocyst pattern. Heterocysts produce cN and PatS. cN diffuses along the strain where, due to the action of the GS/GOGAT cycle (see Fig. 2), decreases the levels of 2-OG breaking the autoregulatory core NtcA-HetR. On the other hand, early during the differentiation, PatS (or other derivative of it, see the text) diffuses along the strain inhibiting HetR. Both processes combined prevent the differentiation of the rest of vegetative cells and explain the formation of the pattern.

The last stages of heterocyst development cause the physiological changes of the cell aimed at creating an anaerobic environment that sustains nitrogen fixation. To this end, two new membrane layers are biosynthesized to decrease the entry of oxygen into the cell [40]. The morphogenesis of these two layers is controlled by two family of genes, *hep* and *hgl*, that are indirectly up-regulated by HetR [33]. After these morphological changes the genes in charge of nitrogen fixation, *nif* genes, are expressed. These genes encode, among others, the nitrogenase enzyme that performs nitrogen fixation.

The fixed nitrogen of the new heterocysts, when transferred to other cells of the strain, acts as an inhibitor of their differentiation together with the transferred PatS [41]. Thus, the diffusion of both PatS and cN from heterocysts along the strain plays a key role in its pattern maintenance (see Fig. 3). Finally, after the differentiation process is finished, a cooperative system between heterocysts and vegetative cells is established so to ensure the survival of the strain. In particular, heterocysts produce fixed nitrogen from N_2 of the atmosphere and they interchange this nitrogen with the oxygen derivatives produced by the vegetative cells.

Regulatory equations

In this section we translate the genetic circuit described previously into a set of differential equations, for which we follow the derivation in [42–44]. Details are left to supplementary information (SI). To simplify notation, constants related to NtcA, HetR, PatS and cN are denoted with the letters a , r , s , and n respectively.

We start looking at the transcription of *ntcA*, which is regulated by HetR and NtcA itself. We assume that the probability that NtcA binds the promoter in the absence of 2-OG can be neglected. Taking into account that both HetR and NtcA dimerize to bind DNA we find:

$$v_a = L_a + \frac{v_a^a \kappa_a^a [2\text{-OG}] [\text{NtcA}]^2 + v_a^r \kappa_a^r [\text{HetR}]^2 + v_a^{ar} \kappa_a^a \kappa_a^r [2\text{-OG}] [\text{NtcA}]^2 [\text{HetR}]^2}{(1 + \kappa_a^a [2\text{-OG}] [\text{NtcA}]^2) (1 + \kappa_a^r [\text{HetR}]^2)}, \quad (1)$$

where v_a measures the production rate of NtcA in units of concentration per time, v_a^a , v_a^r and v_a^{ar} are the rates when only NtcA, only HetR or both are bound to DNA respectively, and κ_*^a are the inverse of the effective dissociation constants of the compounds that bind DNA. On the other hand, L_a , the so-called leak term, measures the basal production of *ntcA* in the absence of regulation. Subscripts and superscripts identify the binding site and the transcription factor for which the constants are given respectively.

Similarly we can obtain the transcription velocity for HetR. We assume that *hetR* is regulated by NtcA by means of a usual Hill function although the real process presents an intermediate, *nrrA*. This

can be done if the mediator element(s) are not regulated through another factor of the genetic circuit under consideration and if they relax rapidly to their limiting values. On the other hand, PatS affects the autoregulatory loop of HetR. It has been suggested that PatS binds the binding site of HetR in the promoter of *hetR* preventing that HetR binds it [33]. These facts, along with the influence of the levels 2-OG, provide with an expression for the transcription velocity:

$$v_r = L_r + \frac{v_r^a \kappa_r^a [2\text{-OG}] [\text{NtcA}]^2 (1 + \kappa_r^s [\text{PatS}]) + v_r^r \kappa_r^r [\text{HetR}]^2 + v_r^{ar} \kappa_r^a \kappa_r^r [2\text{-OG}] [\text{NtcA}]^2 [\text{HetR}]^2}{(1 + \kappa_r^a [2\text{-OG}] [\text{NtcA}]^2) (1 + \kappa_r^r [\text{HetR}]^2 + \kappa_r^s [\text{PatS}])} \quad (2)$$

HetR regulates most processes of the genetic circuit. It governs, among others, the transcription of *ntcA*, *patS*, *hep*, *hgl* and *nif* genes that lead to most of structural changes of the cell and to nitrogen fixation.

The inhibitor PatS is regulated by HetR, and we assume no other influence. This gives the simple transcription velocity:

$$v_s = L_s + \frac{v_s^r \kappa_s^r [\text{HetR}]^2}{1 + \kappa_s^r [\text{HetR}]^2} \quad (3)$$

Finally, we have to relate nitrogenase concentration [Ni] to that of combined Nitrogen [cN], both regulated by HetR and the levels of 2-OG [2-OG]. Let us begin by examining nitrogenase concentration, which is directly controlled by *nif* genes. Although this is not a direct process, we can assume, as we did for the NtcA-regulation by *hetR*, that *nif* genes are functionally governed by [HetR] following a typical Hill function. The nitrogenase production rate is given by:

$$\frac{d[\text{Ni}]}{dt} = L_{Ni} + \frac{v_{Ni}^r \kappa_{Ni}^r [\text{HetR}]^2}{1 + \kappa_{Ni}^r [\text{HetR}]^2} - \delta_{Ni} [\text{Ni}]. \quad (4)$$

where δ_{Ni} represents the degradation rate of nitrogenase. We can effectively account for the lag introduced by intermediate processes not taken into account explicitly in the model by increasing the value of δ_{Ni} so that [Ni] relaxes more slowly. Assuming that nitrogenase produces fixed nitrogen at a constant rate, we arrive at the equation that governs cN levels in cyanobacteria:

$$\frac{d[\text{cN}]}{dt} = L'_n + v'_n [\text{Ni}] - \delta'_n [\text{cN}], \quad (5)$$

where L'_n represents the flux of cN from the exterior of the cell. Assuming that the levels of cN relax rapidly we solve Equation (5) for the steady state. Substituting in Equation (4) we find:

$$\frac{d[\text{cN}]}{dt} = L_n + \frac{v_n^r \kappa_n^r [\text{HetR}]^2}{1 + \kappa_n^r [\text{HetR}]^2} - \delta_n [\text{cN}], \quad (6)$$

where

$$L_n = \frac{1}{\delta_n} (v_n L_{Ni} + \delta_{Ni} L'_n), \quad v_n^r = \frac{v'_n}{\delta'_n} v_{Ni}^r, \quad \delta_n = \delta_{Ni}, \quad \kappa_n^r = \kappa_{Ni}^r. \quad (7)$$

To get a closed system of equations, we shall investigate the relation between cN and 2-OG. Both are related by means of the GS/GOGAT cycle (Fig. 2). Assuming the cycle is in equilibrium and reactions are grounded on the law of mass action, the following two conditions must be satisfied:

$$[\text{glutamate}] = \kappa_{\leftarrow} [\text{glutamine}] [2\text{-OG}], \quad [\text{glutamine}] = \kappa_{\rightarrow} [\text{glutamate}] [\text{cN}], \quad (8)$$

that lead to the relation:

$$[2\text{-OG}] = \frac{1}{\kappa_{\leftarrow} \kappa_{\rightarrow} [\text{cN}]}. \quad (9)$$

Constants			
$l_a = 0.2$	$l_r = 0.01$	$l_s = 0.0001$	$l_n = 0$
$d_a = 0.7$	$d_s = 0.05$	$d_n = 0.01$	$\beta_a^a = 4$
$\beta_a^r = 4$	$\beta_a^{ar} = 8$	$\beta_r^a = 1$	$\beta_r^r = 1$
$\beta_r^{ar} = 3$	$\beta_s^r = 0.385$	$\beta_n^r = 0.06$	$\gamma_a^a = 3$
$\gamma_a^r = 2.4$	$\gamma_s^r = 1.2$	$\gamma_n^r = 2.75$	

Table 1. Parameters for Eq. (11) that reproduce heterocyst formation under noisy conditions and pattern formation when PatS and cN diffuse along a strain of cyanobacteria.

However, this expression does not behave properly for small concentrations of cN, which are expected under cN deprivation: 2-OG levels would increase without limit. In fact, 2-OG production is controlled by some processes that are not considered in this work and so its value must be limited. We can effectively include such a limiting value by means of a translation on [cN] in Eq. (9)

$$[2\text{-OG}] = \frac{1}{\kappa_{2\text{-OG}} + \kappa_{\leftarrow} \kappa_{\rightarrow} [\text{cN}]}, \quad (10)$$

which reaches the maximum value $[2\text{-OG}]_{\max} = 1/\kappa_{2\text{-OG}}$ at $[\text{cN}] = 0$.

Finally we can introduce the differential equations governing cyanobacterial reaction to nitrogen deprivation. They represent the temporal variation of the most important factors of the genetic circuit, namely NtcA, HetR, PatS and cN. Using the production rates (26), (2), (3), (6) and introducing degradation rates constants, δ_* , we find:

$$\begin{aligned} \frac{dq_a}{d\tau} &= l_a + \frac{\beta_a^a \gamma_a^a q_a^2 + \beta_a^r \gamma_a^r q_r^2 (1 + q_n) + \beta_a^{ar} \gamma_a^a q_a^2 \gamma_a^r q_r^2}{(1 + q_n + \gamma_a^a q_a^2)(1 + \gamma_a^r q_r^2)} - d_a q_a, \\ \frac{dq_r}{d\tau} &= l_r + \frac{\beta_r^a q_a^2 (1 + q_s) + \beta_r^r q_r^2 (1 + q_n) + \beta_r^{ar} q_a^2 q_r^2}{(1 + q_n + q_a^2)(1 + q_s + q_r^2)} - q_r, \\ \frac{dq_s}{d\tau} &= l_s + \frac{\beta_s^r \gamma_s^r q_r^2}{1 + \gamma_s^r q_r^2} - d_s q_s, \\ \frac{dq_n}{d\tau} &= l_n + \frac{\beta_n^r \gamma_n^r q_r^2}{1 + \gamma_n^r q_r^2} - d_n q_n, \end{aligned} \quad (11)$$

where we have introduced the adimensional variables:

$$q_a = \underbrace{\sqrt{\frac{\kappa_r^a}{\kappa_{2\text{-OG}}}}}_{\phi_a} [\text{NtcA}], \quad q_r = \underbrace{\sqrt{\kappa_r^r}}_{\phi_r} [\text{HetR}], \quad q_s = \underbrace{\kappa_r^s}_{\phi_s} [\text{PatS}], \quad q_n = \underbrace{\frac{\kappa_{\leftarrow} \kappa_{\rightarrow}}{\kappa_{2\text{-OG}}}}_{\phi_n} [\text{cN}], \quad \tau = \delta_r t, \quad (12)$$

and the constants

$$l_* = \frac{L_* \phi_*}{\delta_r}, \quad \beta_* = \frac{v_* \phi_*}{\delta_r}, \quad \gamma_* = \frac{\kappa_*}{\kappa_r}, \quad d_* = \frac{\delta_*}{\delta_r}. \quad (13)$$

Let us finally stress that this is a *deterministic* model for a single cyanobacterium. The study of the cyanobacterial strain is left to the final section. We advance that the main modification will be adding diffusion processes for the inhibitors PatS and cN through the chain. An important ingredient in pattern formation, noise, will be also added to the equations.

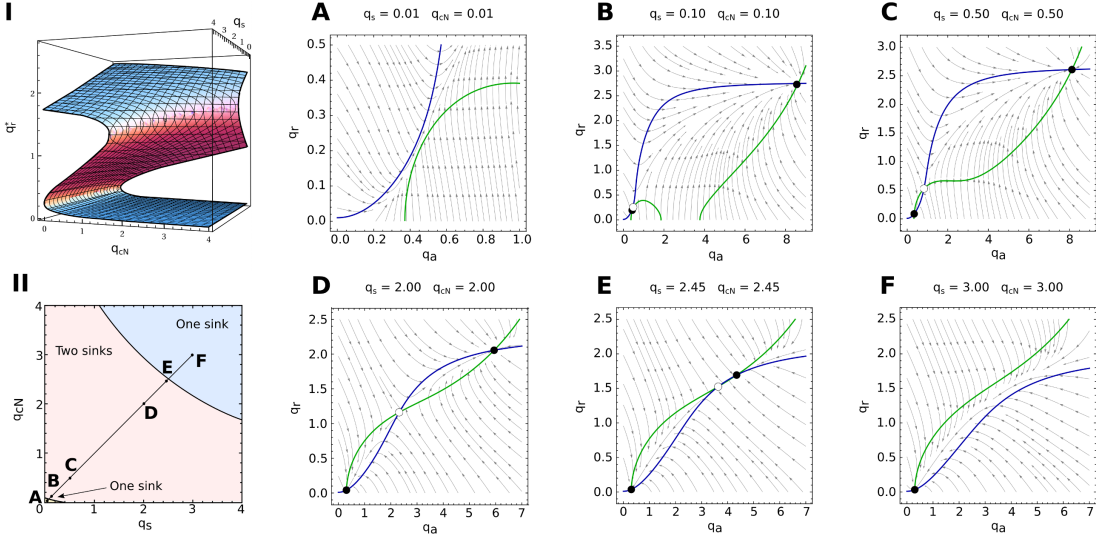


Figure 4. Adiabatic elimination of the fast variables q_r and q_a . Due to the fast dynamics that HetR and NtcA exhibit, we can approach the treatment of the system by adopting a point of view that follows the slower variables q_s and q_n . From this viewpoint, the time-evolution of the pair $(q_s(t), q_n(t))$ is considered by assuming that q_r and q_a instantaneously relax to an equilibrium, which corresponds to a sink (q_r^*, q_a^*) for the fixed pair $(q_s(t), q_n(t))$. Depending on the region of the (q_s, q_n) -plane, there are three fixed points (two sinks corresponding to the highest and the lowest concentrations respectively and a saddle in the middle) or one (a sink) for q_r and q_a (I and II). There are two one-sink regions that are separated from the two-sink region by saddle-node bifurcations (A-F). Sinks and saddles are represented by filled and unfilled circles respectively and arrows indicate the flow of the dynamics. We can then imagine the dynamics of q_s and q_n as evolving either in the bottom or in the top branch of I. In the two-sink region, both branches are plausible and the history of the dynamics determine the solution (hysteresis effect): a dynamics in a branch will continue in it until experiencing a bifurcation in the (q_r, q_a) plane (see Fig. 5 for examples).

Unicellular dynamics

In this section we analyze the dynamical system (11) for a set of constants (Table 1) that exhibit both the dynamical and the structural properties of heterocyst differentiation. Following the usual procedure in the theory of dynamical systems, we study the basic properties of equations (11), such as fixed points and linear stability analysis, so to analyze the key features leading to heterocyst differentiation.

Taking into account the difference between the relaxation times of the constituents of the model, given by the inverses of d_* (see Table 1), we can think it is composed of two temporally separated systems: a rapid one, formed by HetR and NtcA, showing fast dynamics that relaxes to its steady state almost instantaneously and a slow one, composed of PatS and cN, whose evolution is dictated by the values of HetR and NctA in their instantaneous equilibrium. This corresponds to an adiabatic elimination technique [45] that helps in understanding the behavior of the system since it reduces the complexity of the dynamical system by splitting it into two simpler interdependent subsystems.

First, we look for the fixed points of the fast variables q_a and q_r for each pair of values of q_s and q_n

$$f_a(q_s, q_n) = \frac{dq_a}{d\tau} = 0, \quad f_r(q_s, q_n) = \frac{dq_r}{d\tau} = 0. \quad (14)$$

The numerical solution to this problem is sketched in Fig. 4. We find three different branches of solutions

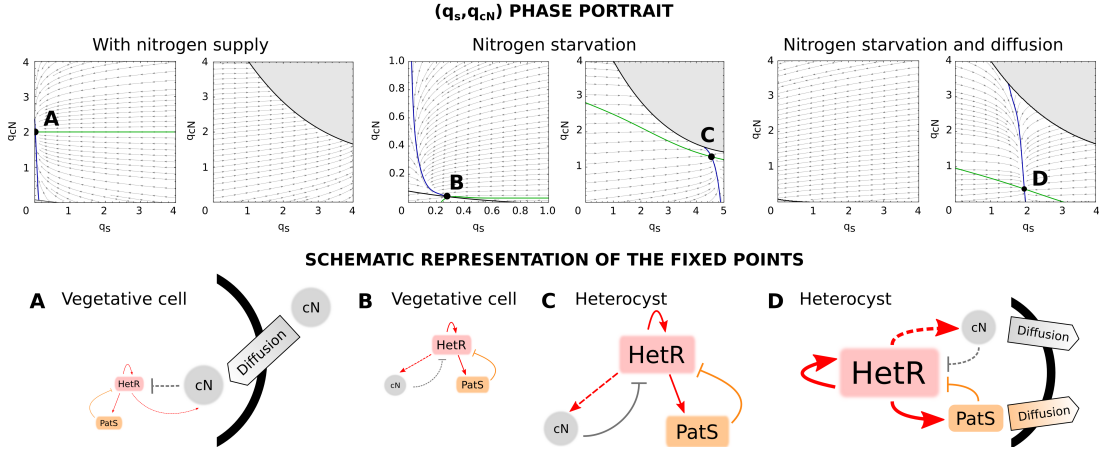


Figure 5. States of a cyanobacterium when subjected to different conditions of nitrogen and diffusion. When the cell is provided of cN ($l_n = 0.03$), there is only one stable fixed point (A) in the bottom branch, which corresponds to a state in which the production of both HetR and PatS is minimum (vegetative-like state). When subjected to nitrogen deprivation ($l_n = 0$), there are two stable fixed points (B and C) each one in a different branch. The first point (B) is a vegetative-like state in which there exists an equilibrium between a small production of HetR, PatS and cN. The same kind of equilibrium is present in the second fixed point (C) but in this case the production of all TFs and cN is high (heterocyst-like steady state). When the cell is exposed to nitrogen stress its trajectory evolves from A to the steady state B and thus it remains vegetative. Assuming some diffusion of cN and PatS from the cell ($l_s = -0.2$ and $l_n = -0.002$), the only stable state (D) corresponds to a heterocyst-like state with high levels of production of HetR, cN and PatS, being the latter transported to the surroundings of the cell.

that coexist in some regions. The fixed points on the lower and upper branches are always stable (blue region in Fig. 4I) and those lying on the middle branch (red region) are saddles. Transitions between the regions with one and three fixed points correspond to saddle-node bifurcations in which the middle branch of solutions coalesce with the lower and the upper one respectively. The basins of attraction of both stable fixed points are separated by the stable manifold of the saddle point (Fig. 4 II).

In the bistable region the system behaves as a switch that can be either OFF in a vegetative-like state (lower branch, with a small production of HetR and NtcA) or ON in a heterocyst-like one (upper branch, with a high production of HetR and NtcA). A sufficiently large perturbation may result in the system crossing the manifold of the saddle and falling into the other stable branch of solutions. The distance between the saddle and the nodes determines the size of the perturbation needed to activate or inactivate the system.

Once (14) is solved, we can apply the solution to calculate the effective field sensed by the (q_s, q_n) pair. In the regions showing bistability the field takes two very different forms, one corresponding to the values of the lower branch and another corresponding to those of the upper one (Fig. 5). We expect a *hysteresis effect*: if initially the dynamics lies on a particular branch it will remain on it unless a fluctuation or a bifurcation makes the system jump to the other branch.

When supplied of cN (Fig. 5A) we find only one stable fixed point that corresponds to a vegetative-like state, since it belongs to the lower branch. The upper branch is completely unstable: all the dynamics lying on it will fall down to the lower branch and eventually be attracted to the vegetative-like sink. The steady state is very robust against perturbations since it is far from the bifurcation region and there is a significant distance to the saddle in the $q_r - q_a$ plane.

By reducing the flow of cN from the exterior of the cell ($l_n = 0$) we find that a stable fixed point appears in the upper branch, a heterocyst-like state, and the vegetative-like state gets closer to the bifurcation region becoming more susceptible to perturbations that can make the system jump to the upper branch. When cN is eliminated from the media the cyanobacterium would evolve from state A to state B in the lower branch until a perturbation pushes it to the upper branch, eventually becoming an heterocyst due to the field acting on that branch (Fig. 5B and C).

Diffusion protects cells in the neighborhood of the newly formed heterocyst to initiate the differentiation: as heterocysts are producers of cN and PatS, the vegetative fixed point of the cells in the neighborhood will move towards an A-like state, thus becoming more stable to perturbations. The heterocyst-like fixed point also becomes more stable due to diffusion, since its production of inhibitors is distributed among other cells (see Fig. 5D).

Strains of cyanobacteria. Heterocyst patterns

In the previous section, we introduced a single cell model for the cyanobacterial reaction to nitrogen-limiting conditions. There we have shown that, for a specific range of parameters, the model exhibits features that would lead to heterocyst development under noisy conditions. Nevertheless, the model should be extended to cyanobacteria chains to account for heterocyst development since, as said above, isolated cyanobacteria do not become heterocysts by themselves; the action of the chain is needed to generate heterocysts.

In this section, we extend the previous results and consider a chain of vegetative cells facing nitrogen deprivation. The main modification is the introduction of diffusion of PatS and cN along the cyanobacteria chain. For this purpose we add to Equation (12) the discrete version of the diffusion equation:

$$\frac{dC_i}{dt} = D_C (C_{i+1} + C_{i-1} - 2C_i). \quad (15)$$

where D_C is called the *diffusion constant* of the element C. Now, it is straightforward to introduce PatS and cN diffusion into the equations. The dynamics of cell i is characterized by the following set of equations:

$$\begin{aligned} \frac{dq_{i,a}}{d\tau} &= l_a + \frac{\beta_a^a \gamma_a^a q_a^2 + \beta_a^r \gamma_a^r q_r^2 (1 + q_n) + \beta_a^{ar} \gamma_a^a q_a^2 \gamma_a^r q_r^2}{(1 + q_n + \gamma_a^a q_a^2)(1 + \gamma_a^r q_r^2)} - d_a q_{i,a} + G_{i,a}(t), \\ \frac{dq_{i,r}}{d\tau} &= l_r + \frac{\beta_r^a q_a^2 (1 + q_s) + \beta_r^r q_r^2 (1 + q_n) + \beta_r^{ar} q_a^2 q_r^2}{(1 + q_n + q_a^2)(1 + q_s + q_r^2)} - q_{i,r} + G_{i,r}(t), \\ \frac{dq_{i,s}}{d\tau} &= l_s + \frac{\beta_s^r \gamma_s^r q_r^2}{1 + K_s^r q_r^2} - d_s q_{i,s} + D_s (q_{i+1,s} + q_{i-1,s} - 2q_{i,s}) + G_{i,s}(t), \\ \frac{dq_{i,n}}{d\tau} &= l_n + \frac{\beta_n^r \gamma_n^r q_r^2}{1 + \gamma_n^r q_r^2} - d_n q_{i,n} + D_n (q_{i+1,n} + q_{i-1,n} - 2q_{i,n}) + G_{i,n}(t), \end{aligned} \quad (16)$$

which constitutes the model for a cyanobacteria strain. To account for environment variability we add white noise, $G_{i,*}(t)$, of the same amplitude, $\langle G_{i,*}(t)G_{i,*}(t') \rangle = \xi \delta(t - t')$, for all the components of the system. Based on these equations, we investigate the conditions that lead to a heterocyst pattern. It is easy to notice that they correspond to an activator-inhibitor system of cells coupled in a reaction-diffusion scheme [46]. This kind of systems produce regular pattern formation [47, 48]. Turing (linear stability) analysis of equations (16) (see SI) provides insight on the periodicity of patterns. It is interesting to show that the minimum periodicity observed in such analysis is larger than 1, which means that a single bacteria is unable to differentiate.

We performed the direct integration of equations (16) for chains of 200 cyanobacteria. We used a Runge-Kutta method for the numerical integration of stochastic differential equations (see Methods) [49]. The level of noise that best reproduces heterocyst pattern is $\xi = 0.001$ for the set of parameters of Table

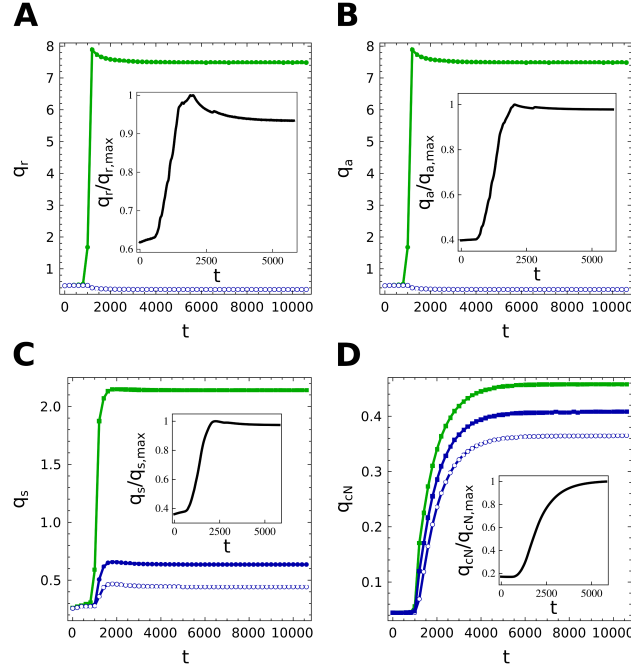


Figure 6. Time evolution of the main components of the differentiation in heterocysts (green) and vegetative cells (blue). Averages along the strain are also presented (black). Heterocysts, due to the early diffusion, evolve toward steady states of the type D of Fig 5 characterized by high levels of HetR and NtcA while vegetative cells present very low concentrations of them (A and B). The levels of PatS and cN in vegetative cells depend on their distance to close heterocysts: C and D show the concentrations of PatS and cN in a heterocyst and in its first two neighbouring vegetative cells, which clearly highlight the effect of diffusion along the strain.

1. Importantly, isolated cells do not initiate differentiation with this level of noise, in agreement with the results from the linear stability analysis. On the other hand, diffusion constants have been set to $D_s = 0.1$ and $D_n = 0.2$. Heterocysts patterns develop for different levels of noise and diffusion constants, but the model parameters, which characterize cell response to nitrogen deprivation, should change accordingly. This correlation between noise, diffusion and model parameters supports the idea that cyanobacteria have evolved towards the better response to the normal levels of noise in their environment.

In Fig. 6 we show the dynamics that the 4 variables exhibit when the chain is deprived of cN. We observe that the chain relaxes to the constant protein levels of the vegetative-like state we showed in the previous chapter. Then, due to the coupled action of noise and diffusion, some cells start to differentiate. As new forming heterocysts appear, their production and exportation of inhibitors to the surrounding cells make the latter more stable to perturbations stopping their differentiation. The model reproduces very well the initial peak that both NtcA and HetR present experimentally [33, 50]. PatS increases more slowly to its steady value reducing the levels of NtcA and HetR and, finally, cN is generated by heterocysts stabilizing the pattern.

Fig. 7 shows the evolution of the profile for a 200 cells chain of cyanobacteria. We observe that heterocysts progressively appear in those regions in which others heterocysts do not have effect (*i.e.* those vegetative cells that are not supplied of sufficient cN and PatS). Finally, a semiregular pattern is generated. PatS and cN diffuse along the strain exhibiting smooth variations between vegetative cells and heterocysts, while HetR and NtcA present very abrupt variations between cell types.

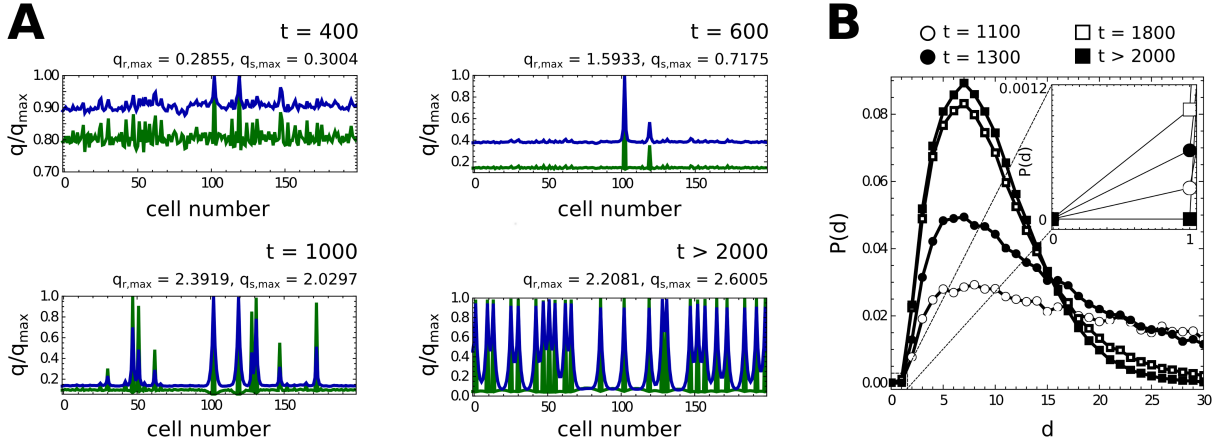


Figure 7. Time-evolution of the pattern of heterocysts (A) and of the probability distribution of the distance between consecutive heterocysts (B). Green and blue curves represent the concentration profiles of HetR and PatS (NtcA and cN are not presented since their behavior along the strain is comparable to the one of HetR and PatS, see Fig. 6 to see the similarities). Small perturbations along the strain of vegetative cells (initially in the steady state B of Fig. 5) are amplified due to diffusion processes in a demonstration of Turing’s theory [47]. New heterocysts appear in regions that are not dominated by the action of other heterocysts. Finally, the competition between nearby differentiating cells ceases the differentiation of some of them, as observed in B: consecutive heterocysts, which are created by strong perturbations, finally disappear due to the aforementioned competition. The final pattern presents localized levels of HetR (heterocysts) and a diffusive-like behavior of PatS, as it was expected.

Finally, in Fig. 7.B we show the time-evolution of the histogram for the distance between two consecutive heterocysts. It should be stressed that although initially some close heterocysts appear, they are eliminated by the non-linear action of the system during the differentiation process. Close heterocysts compete for the same region of action (the same vegetative cells that consume their PatS and cN) and then they cannot reach the optimal heterocyst-like state, which is stable to slight perturbations. Finally, one of them falls down from the upper branch becoming a vegetative cell. This behavior is typically observed experimentally [4,9]. The final histogram can be nicely fitted by a Γ -distribution.

Discussion

The study of cell differentiation and its underlying mechanisms constitutes one of most intriguing problems in biology. This phenomena is the basis for multicellular organism and pattern formation. The approach we have chosen in this paper is to deal with a simple system, the heterocyst formation in cyanobacteria strains, yet complex enough to capture the main ingredients of some of the mechanism for cell differentiation and pattern formation under external driving. The knowledge of the basic regulatory genes and their corresponding interactions allows for a detailed description of cell dynamics. We have proposed the dynamical equations for these regulatory genes based in the statistical mechanics of the regulation process. This allow us to obtain a detailed description of the *continuous time dynamics* of the main regulatory protein, in contrast to other discrete approximations based in boolean dynamics [13]. This kind of analysis have been proved successfully in other time dependent phenomena in the cyanobacterial world like circadian cycles [51]. The analysis of the "unicellular dynamics" has revealed that the two cellular stable states, vegetative and heterocyst cells, appear as attractors of the non-linear dynamics of the regulation equations. However, the study of many coupled cells is needed as cyanobacteria do not

differentiate when isolated.

The model is thus completed by coupling a number of cells in a one-dimensional array so that combined nitrogen and PatS can diffuse along the chain of cells. One important ingredient affecting the dynamical behavior of the chain is noise, which appears to have a key role in the transition from the initial chain of vegetative cells to the steady state in which heterocysts coexist with vegetative cyanobacteria. Thus, the appearance of differentiation is, in our model, a pure stochastic event. The cooperative character of the strain is clear from the amount of noise needed to start the differentiation process which appears significantly smaller than that needed in isolated cells. The source of noise as well as its biological consequences is, nowadays a current topic of research [52]. In fact, at its initial state, differentiation of cells appear randomly along the strain, but shortly after its onset a characteristic distribution of heterocyst emerges. This distribution can be compared with the experimental one with a fairly agreement [39].

Although the model presented here integrates both internal cell dynamics and the coupling between cells via diffusion, there exist other ingredients that can also be incorporated. One issue that have not been considered in this work is the possibility of replication of vegetative cells. This effect has been taken into account in [12]. Although this improvement is relevant, it only affects, in our approach, to the mean separation between heterocysts, by opening a gap in the Γ -function shaped of Fig. 6B and thus approaching better to the experimental distribution.

Other improvements to the approach presented here will come from the availability of more experimental data. Unlike other approaches [11] where comparison is done (globally) with heterocyst distributions, our work would allow for a qualitative comparison of each component involved in the differentiation (see Fig. 6). Unfortunately, experimental data are not enough to make a detailed fit and then extract reliable parameters. The availability of such data is extremely important both for having better set of model parameters and to validate new models. A complete understanding of the mechanism that derive in phenotypic differentiation is the first step for a modular comprehension of the whole cell [53].

Methods

To reproduce the dynamics of Eq. (16) we make use of the integration scheme proposed in [49]. Eq. (16) is a set of stochastic differential equations (SDE) so its numerical integration requires generating a statistical representative trajectory for a discrete set of time-values. A SDE of the form

$$\dot{x} = f(x) + G(t), \quad (17)$$

where $G(t)$ is a Gaussian white noise with

$$\langle G(t) \rangle = 0, \text{ and, } \langle G(t)G(t') \rangle = \xi\delta(t' - t),$$

can be integrated through a Runge-Kutta integration algorithm by adding a particular Gaussian signal at each stage of the scheme. This algorithm coincides with the usual Runge-Kutta scheme for $\xi = 0$. In this work we have employed a $3O4S2G$ algorithm, which is correct up to 3^{th} order, is developed in 4 stages and uses 2 independent Gaussian random variables.

Acknowledgments

We acknowledge financial support from the Spanish MINECO under projects FIS2011-25167 and FIS2012-38266-C02-01. J.G.G. is supported by the Spanish MINECO through the Ramon y Cajal program. We are grateful to S. Ares and J. Muñoz-García for sharing ideas and useful discussions. We also acknowledge the "Genetic Regulation and Physiology of Cyanobacteria" group at University of Zaragoza for sharing insight on the genetic of heterocyst formation.

References

1. Koch A, Meinhardt H (1994) Biological pattern formation: from basic mechanisms to complex structures. *Rev Mod Phys* 66: 1481–1511.
2. Süel GM, Garcia-Ojalvo J, Liberman LM, Elowitz MB (2006) An excitable gene regulatory circuit induces transient cellular differentiation. *Nature* 440: 545–550.
3. Wolk C (1998) Heterocyst formation. *Annu Rev Genet* 30: 59–78.
4. Flores E, Herrero A (2010) Compartmentalized function through cell differentiation in filamentous cyanobacteria. *Nature Rev* 8: 39–50.
5. Schirrmeister B, Antonelli A, Bagheri H (2011) The origin of multicellularity in cyanobacteria. *BMC Evol Biol* 11: 45.
6. Shi Y, Zhao W, Zhang W, Ye Z, Zhao J (2006) Regulation of intracellular free calcium concentration during heterocyst differentiation by HetR and NtcA in *Anabaena* sp. PCC7120. *Proc Nat Acad Sci (USA)* 103: 11334–11339.
7. Toepel J, Welsh E, Summerfield T, Pakrasi H, Sherman L (2008) Differential Transcriptional Analysis of the Cyanobacterium *Cyanothece* sp. Strain ATCC 51142 during Light-Dark and Continuous-Light Growth. *J Bacteriol* 190: 3904–3913.
8. Yoon H (1998) Heterocyst Pattern Formation Controlled by a Diffusible Peptide. *Science* 282: 935–938.
9. Zhang CC, Laurent S, Sakr S, Peng L, Bédu S (2006) Heterocyst differentiation and pattern formation in cyanobacteria: a chorus of signals. *Mol microbiol* 59: 367–375.
10. Kumar K, Mella-Herrera R, Golden J (2010) Cyanobacterial heterocysts. *Cold Spring Harb Perspect Biol* 2: a000315.
11. Allard J, Hill A, Rutenberg A (2007) Heterocyst patterns without patterning proteins in cyanobacterial filaments. *Dev Biol* 312: 427–434.
12. Brown A, Rutenberg A (2012) Reconciling cyanobacterial fixed-nitrogen distributions and transport experiments with quantitative modelling. *Phys Biol* 9: 016007.
13. Gedtzen Z, Salgado J, Osses A, Asenjo J, Rapaport I, et al. (2009) Modeling heterocyst pattern formation in cyanobacteria. *BMC Bioinf* 10: S16.
14. Laurent S, Chen H, Bédu S, Ziarelli F, Peng L, et al. (2005) Nonmetabolizable analogue of 2-oxoglutarate elicits heterocyst differentiation under repressive conditions in *Anabaena* sp. PCC 7120. *P Natl Acad Sci USA* 102: 9907–9912.
15. Muro-Pastor MI, Reyes JC, Florencio FJ (2001) Cyanobacteria perceive nitrogen status by sensing intracellular 2-oxoglutarate levels. *J Biol Chem* 276: 38320–38328.
16. Vázquez-Bermúdez MF, Herrero A, Flores E (2003) Carbon supply and 2-oxoglutarate effects on expression of nitrate reductase and nitrogen-regulated genes in *Synechococcus* sp. strain PCC 7942. *FEMS Microbiol Lett* 221: 155–159.
17. Muro-Pastor MI, Reyes JC, Florencio FJ (2005) Ammonium assimilation in cyanobacteria. *Photosynth Res* 83: 135–150.

18. Wei TF, Ramasubramanian TS, Golden JW (1994) *Anabaena* sp. strain PCC 7120 *ntcA* gene required for growth on nitrate and heterocyst development. *J Bacteriol* 176: 4473–4482.
19. Frías JE, Flores E, Herrero A (1994) Requirement of the regulatory protein NtcA for the expression of nitrogen assimilation and heterocyst development genes in the cyanobacterium *Anabaena* sp. PCC 7120. *Mol microbiol* 14(4): 823–832.
20. Vázquez-Bermúdez MF, Herrero A, Flores E (2002) 2-Oxoglutarate increases the binding affinity of the NtcA (nitrogen control) transcription factor for the *Synechococcus glnA* promoter. *FEBS lett* 512: 71–74.
21. Tanigawa R, Shirokane M, Maeda Si Si, Omata T, Tanaka K, et al. (2002) Transcriptional activation of NtcA-dependent promoters of *Synechococcus* sp. PCC 7942 by 2-oxoglutarate in vitro. *P Natl Acad Sci USA* 99: 4251–4255.
22. Ramasubramanian TS, Wei TF, Oldham aK, Golden JW (1996) Transcription of the *Anabaena* sp. strain PCC 7120 *ntcA* gene: multiple transcripts and NtcA binding. *J Bacteriol* 178: 922–926.
23. Ramasubramanian TS, Wei TF, Golden JW (1994) Two *Anabaena* sp. strain PCC 7120 DNA-binding factors interact with vegetative cell- and heterocyst-specific genes. *J Bacteriol* 176: 1214–1223.
24. Buikema WJ, Haselkorn R (1991) Isolation and complementation of nitrogen fixation mutants of the cyanobacterium *Anabaena* sp. strain PCC 7120. *J Bacteriol* 173: 1879–1885.
25. Buikema WJ, Haselkorn R (1991) Characterization of a gene controlling heterocyst differentiation in the cyanobacterium *Anabaena* 7120. *Gene Dev* 5: 321–330.
26. Ehira S, Ohmori M (2006) NrrA directly regulates expression of *hetR* during heterocyst differentiation in the cyanobacterium *Anabaena* sp. strain PCC 7120. *J Bacteriol* 188: 8520–8525.
27. Wisén S, Jiang F, Bergman B, Mannervik B (1999) Expression and purification of the transcription factor NtcA from the cyanobacterium *Anabaena* PCC 7120. *Protein expres purif* 17: 351–357.
28. Alfonso M, Kirilovsky D (2001) Redox Control of *ntcA* Gene Expression in *Synechocystis* sp . PCC 6803 . Nitrogen Availability and NtcA Protein 1. *Plant Physiol* 125: 969–981.
29. Li JH (2003) An increase in the level of 2-oxoglutarate promotes heterocyst development in the cyanobacterium *Anabaena* sp. strain PCC 7120. *Microbiology* 149: 3257–3263.
30. Buikema WJ, Haselkorn R (2001) Expression of the *Anabaena hetR* gene from a copper-regulated promoter leads to heterocyst differentiation under repressing conditions. *P Natl Acad Sci USA* 98: 2729–2734.
31. Khudyakov IY, Golden JW (2004) Different functions of HetR, a master regulator of heterocyst differentiation in *Anabaena* sp. PCC 7120, can be separated by mutation. *P Natl Acad Sci USA* 101: 16040–16045.
32. Zhou R, Wei X, Jiang N, Li H, Dong Y, et al. (1998) Evidence that HetR protein is an unusual serine-type protease. *P Natl Acad Sci USA* 95: 4959–4963.
33. Huang X, Dong Y, Zhao J (2004) HetR homodimer is a DNA-binding protein required for heterocyst differentiation, and the DNA-binding activity is inhibited by PatS. *P Natl Acad Sci USA* 101: 4848–4853.

34. Muro-Pastor AM, Valladares A, Flores E, Herrero A (2002) Mutual dependence of the expression of the cell differentiation regulatory protein HetR and the global nitrogen regulator NtcA during heterocyst development. *Mol microbiol* 44: 1377–1385.
35. Valladares A, Muro-pastor AM, Herrero A, Flores E (2004) The NtcA-Dependent P 1 Promoter Is Utilized for *glnA* Expression in N₂-Fixing Heterocysts of *Anabaena* sp . Strain PCC 7120. *J Bacteriol* 186: 7337–7343.
36. Fiedler G, Muro-Pastor A (2001) NtcA-Dependent Expression of the *devBCA* Operon, Encoding a Heterocyst-Specific ATP-Binding Cassette Transporter in *Anabaena* spp. *J Bacteriol* 183: 3795–3799.
37. Hebbar PB, Curtis SE (2000) Characterization of *devH*, a gene encoding a putative DNA binding protein required for heterocyst function in *Anabaena* sp. strain PCC 7120. *J Bacteriol* 182: 3572–3581.
38. Wu X, Liu D, Lee MH, James W, Golden JW (2004) *patS* Minigenes Inhibit Heterocyst Development of *Anabaena* sp . Strain PCC 7120 *patS* Minigenes Inhibit Heterocyst Development of *Anabaena* sp . Strain PCC 7120. *J Bacteriol* 186: 6422–6429.
39. Yoon Hs, Golden JW (2001) PatS and Products of Nitrogen Fixation Control Heterocyst Pattern PatS and Products of Nitrogen Fixation Control Heterocyst Pattern. *J Bacteriol* 183: 2605–2613.
40. Fay P (1992) Oxygen relations of nitrogen fixation in cyanobacteria. *Microbiol Rev* 56: 340–373.
41. Wolk CP, Austin SAMM, Bortins J, Galonsky A (1974) Autoradiographic localization of ¹³N after fixation of ¹³N-labeled nitrogen gas by a heterocyst-forming blue-green alga. *J Cell Biol* 61: 440–453.
42. Buchler NE, Gerland U, Hwa T (2003) On schemes of combinatorial transcription logic. *Proc Natl Acad Sci* 100: 5136–5141.
43. Bintu L, Buchler N, Garcia H, Gerland U, Hwa T, et al. (2005) Transcriptional regulation by the numbers: models. *Current opinion in genetics & development* 15: 116–124.
44. Phillips R, Kondev J, Theriot J, Garcia H (2012) *Physical Biology of the Cell*. New York: Garland Science, second edition.
45. Manneville P (1990) *Dissipative structures and weak turbulence*. London: Academic Press.
46. Morelli LG, Uriu K, Ares S, Oates AC (2013) Computational Approaches to Developmental Patterning. *Science* 336: 187–191.
47. Turing AM (1952) The Chemical Basis of Morphogenesis. *Philos Trans R Soc London Ser B* 237: 37–62.
48. Meinhardt H (1982) *Models of Biological Pattern Formation*. London: Academic Press.
49. Greenside, HS and Helfand, E (1981) Numerical-Integration of Stochastic Differential Equations 2. *Bell System Technical Journal* 60: 1927–1940.
50. Jang J, Shi L, Tan H, Janicki A, Zhang CC (2009) Mutual Regulation of *ntcA* and *hetR* during Heterocyst Differentiation Requires Two Similar PP2C-Type Protein Phosphatases, PrpJ1 and PrpJ2, in *Anabaena* sp Strain PCC 7120. *J Bacteriol* 191: 6059–6066.
51. Teng SW, Mukherji S, Moffitt JR, de Buyl S, OShea EK (2013) Robust circadian oscillations in growing cyanobacteria require transcriptional feedback. *Science* 340: 737–740.

52. Suel GM, Kulkarni RP, Dworkin J, Garcia-Ojalvo J, Elowitz MB (2007) Tunability and noise dependence in differentiation dynamics. *Science* 315: 1716-1719.
53. Karr J, Sanghvi J, Macklin D, Gutschow M, Jacobs J, et al. (2012) A whole-cell computational model predicts phenotype from genotype. *Cell* 150: 389 - 401.

Supporting Information

Regulatory equations: a statistical mechanics approach

To derive the equations regulating transcription processes during heterocyst differentiation, we follow an approach similar to the detailed in [42–44]. This is a thermodynamic approach to transcription in which binding sites are considered two-states systems, either empty or containing a binding protein. The probability that a given transcription factor (TF) is bound to its binding site is given by the Arrhenius formula

$$p_{\text{TF}} = \frac{[\text{TF}]K_{\text{TF}}}{1 + [\text{TF}]K_{\text{TF}}} = \frac{q_{\text{TF}}}{1 + q_{\text{TF}}} \quad (18)$$

where $[\text{TF}]$ is the concentration of the TF, K_{TF} is the inverse of the effective dissociation constant, which represents the concentration of half-maximal occupation, and $q_{\text{TF}} = [\text{TF}]K_{\text{TF}}$ is called the binding affinity. The denominator of Eq. (18) is nothing but the canonical partition function of the promoter $Z = 1 + [\text{TF}]K_{\text{TF}}$, representing the Boltzmann-weighted sum of possible states of the binding site. Transcription starts with the binding of RNAP, which in the absence of interactions with TFs follows the probability law of Eq. (18):

$$p_{\text{RNAP}} = \frac{q_{\text{RNAP}}}{1 + q_{\text{RNAP}}} \quad (19)$$

Let us examine the case in which RNAP interacts with a TF within the promoter. In this case the partition function is

$$Z_{\text{RNAP,TF}} = 1 + [\text{TF}]K_{\text{TF}} + [\text{RNAP}]K_{\text{RNAP}} + [\text{RNAP}][\text{TF}]K_{\text{RNAP,TF}} \quad (20)$$

with $K_{\text{RNAP,TF}}$ the inverse dissociation constant of the complex RNAP&TF that can be higher than $K_{\text{TF}}K_{\text{RNAP}}$ if the interaction of the two proteins within the promoter is attractive or smaller if the interaction is repulsive. In the first case we say that the TF is an inhibitor while in the second case we say that the TF is an activator. We are interested in the probability that RNAP is bound to its binding site. This probability is

$$\begin{aligned} p_{\text{RNAP}} &= \frac{[\text{RNAP}]K_{\text{RNAP}} + [\text{RNAP}][\text{TF}]K_{\text{RNAP,TF}}}{1 + [\text{TF}]K_{\text{TF}} + [\text{RNAP}]K_{\text{RNAP}} + [\text{RNAP}][\text{TF}]K_{\text{RNAP,TF}}} = \\ &= \frac{q_{\text{RNAP}}(1 + q_{\text{TF}}\omega_{\text{RNAP,TF}})}{1 + q_{\text{TF}} + q_{\text{RNAP}}(1 + q_{\text{TF}}\omega_{\text{RNAP,TF}})}, \end{aligned} \quad (21)$$

where we have used the definitions $q_{\text{TF}} = [\text{TF}]K_{\text{TF}}$, $q_{\text{RNAP}} = [\text{RNAP}]K_{\text{RNAP}}$ and $\omega_{\text{RNAP,TF}} = K_{\text{RNAP,TF}}/(K_{\text{TF}}K_{\text{RNAP}})$. Now, assuming that $[\text{RNAP}]$ does not vary during the transcription process (or that it is not the limiting factor of transcription) and that transcription (which we remind is nothing but the production of mRNA) takes place at a given velocity ν when RNAP is bound to the promoter, we can find the relation between q_{TF} and the transcription velocity v_{mRNA} :

$$v_{\text{mRNA}} = L^A + v_{\text{TF}} \frac{q_{\text{TF}}\kappa_{\text{TF}}^A}{1 + q_{\text{TF}}\kappa_{\text{TF}}^A}, \quad (22)$$

for the case in which the TF is an activator ($\omega_{\text{RNAp,TF}} > 1$) or

$$v_{\text{mRNA}} = L^I + v_{\text{TF}} \frac{1}{1 + q_{\text{TF}} \kappa^I}, \quad (23)$$

in the case of an inhibitor ($\omega_{\text{RNAp,TF}} < 1$). The remaining constants are

$$\begin{aligned} v_{\text{TF}} &= \nu \frac{q_{\text{RNAp}} |\omega_{\text{RNAp,TF}} - 1|}{(1 + q_{\text{RNAp}})(1 + q_{\text{RNAp}} \omega_{\text{RNAp,TF}})}, \\ \kappa^A &= \frac{1}{\kappa^I} = \frac{1 + \omega_{\text{RNAp,TF}} q_{\text{RNAp}}}{1 + q_{\text{RNAp}}}, \\ L_{\text{mRNA}}^A &= \nu \frac{q_{\text{RNAp}}}{1 + q_{\text{RNAp}}}, \\ L_{\text{mRNA}}^I &= \nu \frac{q_{\text{RNAp}} \omega_{\text{RNAp,TF}}}{1 + q_{\text{RNAp}} \omega_{\text{RNAp,TF}}}. \end{aligned} \quad (24)$$

These equations are of the form of the Michaelis-Menten equations of reaction kinetics with a leak term, represented by L^A or L^I depending on the case, that stands for the production of mRNA in the absence of regulation. This example shows the main features of the statistical mechanics approach to transcription. More complex transcription processes can be dealt with in a similar way by computing their corresponding partition function and counting the RNAp-active states.

For all processes in the article we assume that TFs do not interact within the promoter but rather that they cooperatively affect the velocity at which transcription takes place. This is the simplest way in which we can consider the interaction between different TFs and, on the other hand, it is rich enough to represent the main features of the transcription processes we need to account for.

Let us sketch, for instance, the regulation of *ntcA* in heterocyst development (see main text). *ntcA* is regulated partly by NtcA (in its dimer configuration) and 2-OG and also by HetR. The partition function in this case is:

$$\begin{aligned} Z_{\text{RNAp,NtcA\&2-OG,HetR}} &= 1 + [\text{RNAp}] K_{\text{RNAp}} + [\text{NtcA}]^2 [2\text{-OG}] K_{\text{NtcA2,2-OG}} + \\ &+ [\text{RNAp}] [\text{NtcA}]^2 [2\text{-OG}] K_{\text{RNAp,NtcA2,2-OG}} \\ &+ [\text{HetR}]^2 K_{\text{HetR2}} + [\text{RNAp}] [\text{HetR}]^2 K_{\text{RNAp,HetR2}} + \\ &+ [\text{HetR}]^2 [\text{NtcA}]^2 [2\text{-OG}] K_{\text{NtcA2,2-OG}} K_{\text{HetR2}} \\ &+ [\text{RNAp}] [\text{HetR}]^2 [\text{NtcA}]^2 [2\text{-OG}] K_{\text{RNAp,NtcA2,2-OG}} K_{\text{RNAp,HetR2}} \end{aligned} \quad (25)$$

Both NtcA and HetR acts as activators, and we finally arrive to the transcription velocity

$$v_a = L_a + \frac{v_a^a \kappa_a^a [2\text{-OG}] [\text{NtcA}]^2 + v_a^r \kappa_a^r [\text{HetR}]^2 + v_a^{ar} \kappa_a^a \kappa_a^r [2\text{-OG}] [\text{NtcA}]^2 [\text{HetR}]^2}{(1 + \kappa_a^a [2\text{-OG}] [\text{NtcA}]^2)(1 + \kappa_a^r [\text{HetR}]^2)} \quad (26)$$

where v_a^a , v_a^r and v_a^{ar} represent the effective transcription velocity when NtcA, HetR or both are bound to DNA respectively. The constants κ are obtained from K by eliminating q_{RNAp} from the equations following a procedure similar to that of Eq. (22) and can be thought as the inverse of effective dissociation constants associated with the binding of the different compounds.

Finally, we consider translation (the process by which mRNA is transformed into the corresponding protein) is produced at a constant rate η per mole of mRNA. Therefore, the concentration of a given TF is given by:

$$\frac{d[\text{TF}]}{dt} = \eta_{\text{TF}} [\text{mRNA}_{\text{TF}}] - \delta_{\text{TF}} [\text{TF}], \quad (27)$$

with δ_{TF} the inverse of the mean lifetime of the TF. On the other hand, the dynamics for concentration of mRNA is

$$\frac{d[\text{mRNA}_{\text{TF}}]}{dt} = v_{\text{mRNA}_{\text{TF}}} - \delta_{\text{mRNA}_{\text{TF}}}[\text{mRNA}_{\text{TF}}], \quad (28)$$

with $\delta_{\text{mRNA}_{\text{TF}}}$ the inverse of the mean lifetime of the mRNA. Usually, $\delta_{\text{mRNA}_{\text{TF}}} \gg \delta_{\text{TF}}$ and, as we are interested in [TF], we can assume that from the viewpoint of the characteristic dynamics of the TF, [mRNA] relaxes instantaneously to its equilibrium value:

$$[\text{mRNA}_{\text{TF}}] = \frac{v_{\text{mRNA}_{\text{TF}}}}{\delta_{\text{mRNA}_{\text{TF}}}}, \quad (29)$$

so

$$\frac{d[\text{TF}]}{dt} = \eta \frac{v_{\text{mRNA}_{\text{TF}}}}{\delta_{\text{mRNA}_{\text{TF}}}} - \delta_{\text{TF}}[\text{TF}]. \quad (30)$$

In an abuse of notation, we redefine the variables v_*^\bullet and l_*^\bullet as $v_*^\bullet \eta_* / \delta_{\text{mRNA}_*}$ and $v_*^\bullet \eta_* / \delta_{\text{mRNA}_*}$ respectively to express the effective constants in Eq. (30). For instance, we find

$$\frac{d[\text{NtcA}]}{dt} = L_a + \frac{v_a^a \kappa_a^a [2\text{-OG}][\text{NtcA}]^2 + v_a^r \kappa_a^r [\text{HetR}]^2 + v_a^{ar} \kappa_a^a \kappa_a^r [2\text{-OG}][\text{NtcA}]^2 [\text{HetR}]^2}{(1 + \kappa_a^a [2\text{-OG}][\text{NtcA}]^2)(1 + \kappa_a^r [\text{HetR}]^2)} - \delta_a [\text{NtcA}] \quad (31)$$

Turing linear stability analysis

Here we discuss the Turing stability analysis of our system [?, ?]. Let us first discuss the general theory. We consider a chain composed of n -dimensional dynamical systems, each one $i = 1, \dots, n$ characterized by $\dot{\mathbf{q}}_i = \mathbf{f}(\mathbf{q}_i)$. If we add diffusion along the chain, the behavior of cell i is characterized by:

$$\frac{d\mathbf{q}_i}{d\tau} = \mathbf{f}(\mathbf{q}_i) + \tilde{D}(\mathbf{q}_{i+1} + \mathbf{q}_{i-1} - 2\mathbf{q}_i), \quad (32)$$

where \tilde{D} is the *diffusion tensor*. Now we consider a (stable) fixed point, \mathbf{q}_0 , of the dynamical system, i.e. $\mathbf{f}(\mathbf{q}_0) = \mathbf{0}$. It also constitutes a fixed point for the entire chain since diffusion terms cancel ($\mathbf{q}_i = \mathbf{q}_j$ for all i and j). We want to analyze the effect of a small perturbation, Δ , around the steady state of the chain. Introducing the variables

$$\mathbf{q}_i = \mathbf{q}_0 + \Delta_i, \quad (33)$$

into Equation 32, and expanding up to first order in Δ one gets:

$$\frac{d\Delta_i}{d\tau} = \nabla \mathbf{f}(\mathbf{q}_0) \cdot \Delta_i + \tilde{D}(\Delta_{i+1} + \Delta_{i-1} - 2\Delta_i), \quad (34)$$

where $\nabla \mathbf{f}(\mathbf{q}_0)$ is the Jacobian matrix of the field evaluated in the point \mathbf{q}_0 . Furthermore, we can decompose the perturbation in terms of plane waves:

$$\begin{aligned} \Delta_i(\tau) &= \sum_k \Delta_{i,k}, \\ \Delta_{i,k}(\tau) &= \mathbf{A} e^{\omega_k \tau} \cos(ki). \end{aligned} \quad (35)$$

The admissible values of the wavevector k depend on the length of the chain and on the boundary conditions. For instance, $k = n\pi/L$ with $n = 1, 2, 3, \dots, L$ for Von Neumann (zero flux) boundary conditions. Introducing 35 into 34 we find:

$$\omega_k \mathbf{A} = \nabla \mathbf{f}(\mathbf{q}_0) \mathbf{A} + 2\tilde{D} \mathbf{A} (\cos k - 1), \quad (36)$$

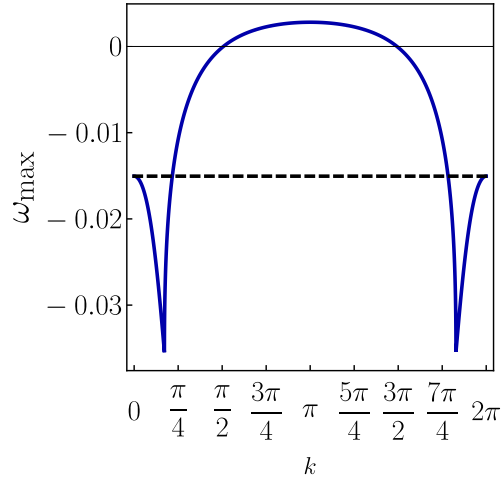


Figure 8. Results for ω_{\max} extracted from Equation 37 for the cyanobacterial system with $D_s = 0.1$ and $D_n = 0.2$ (Blue). The black dashed line indicates the value at equilibrium in the absence of diffusion

which has nontrivial solutions if

$$\det(\nabla \mathbf{f}(\mathbf{q}_0) + 2\tilde{D}(\cos k - 1) - \omega_k) = 0. \quad (37)$$

Therefore, the k mode is related to some possible frequencies ω_k . If those frequencies satisfy $\text{Re}(\omega_k) < 0$, it is expected that the perturbation Δ will be damped (negative exponential) and the system will recover its initial equilibrium. Nevertheless, if $\text{Re}(\omega_k) > 0$ perturbations will be amplified (positive exponential) and thus it is expected that structures of wavelength $2\pi/k$ will develop. The important value that determines if the system is stable to perturbations of some wavevector k is the largest real part of the ω_k from 37.

We can now turn to our cyanobacteria chain characterized by Eq. (16) of the main text. We analyze the effect of perturbations around the vegetative-like state for $D_s = 0.1$ and $D_n = 0.2$ (Figure 8). We find that the system is unstable against perturbations of intermediate wavevectors, with an upper bound (representing a minimum length at which patterns can be formed) and a lower bound (maximum length). The value of the minimum length (measured in cell number) $l_{\min} \approx 8/7 > 1$ so that a single cell is unable to differentiate.